[2+2] versus [3+2] Addition of Metal Oxides Across C═C Double Bonds: Toward an Understanding of the Surprising Chemo- and Periselectivity of Transition-Metal-Oxide Additions to Ketene†

Dirk V. Deubel,* Sabine Schlecht, and Gernot Frenking*

Contribution by the Fachbereich Chemie, Philipps-Universität Marburg, Hans-Meerwein-Strasse, D-35032 Marburg, Germany, and Department of Chemistry, University of Calgary, Calgary, Alberta, Canada T2N 1N4

Received October 20, 2000

Abstract: The peri-, chemo-, stereo-, and regioselectivity of the addition of the transition-metal oxides OsO_4 and $LReO_3$ (L = O^-, H_3PN, Me, Cp) to ketene were systematically investigated using density-functional methods. While metal-oxide additions to *ethylene* have recently been reported to follow a [3+2] mechanism only, the calculations reveal a strong influence of the metal on the periselectivity of the *ketene* addition: OsO_4 again prefers a [3+2] pathway across the C═C moiety whereas, for the rhenium oxides $LReO_3$, the [2+2] barriers are lowest. Furthermore, a divergent chemoselectivity arising from the ligand L was found: ReO_4^- and $(H_3PN)ReO_3$ add across the C═O bond while $MeReO_3$ and $CpReO_3$ favor the addition across the C═C moiety. The calculated energy profile for the $MeReO_3$ additions differs from the $CpReO_3$ energy profile by up to 45 kcal/mol due to the stereoelectronic flexibility of the Cp ligand adopting η^5, η^3, and η^1 bonding modes. The selectivity of the cycloadditions was rationalized by the analysis of donor−acceptor interactions in the transition states. In contrast, metal-oxide additions to *diphenylketene* probably follow a different mechanism: We give theoretical evidence for a zwitterionic intermediate that is formed by nucleophilic attack at the carbonyl moiety and undergoes a subsequent cyclization yielding the thermodynamically favored product. This two-step pathway is in agreement with the results of recent experimental work.

Introduction

The addition of osmium tetraoxide across the C═C double bond of olefins yielding a metalla-2,5-dioxolane is the initial step of *cis*-dihydroxylation, one of the most elegant reactions for a 1,2-functionalization of alkenes.[1,2] The long-standing controversy[3] about the mechanism of the reaction of OsO_4 with olefins has recently been settled by four independent groups with the help of quantum-chemical methods.[4] The reaction does not proceed via an intermediate metalla-2-oxetane[5] formed in a [2+2] cycloaddition but follows a concerted [3+2] pathway (Scheme 1).[6] Elaborated kinetic investigations[7] on the Cp*ReO_3 addition to olefins and the reverse reaction[8,9] were interpreted in favor of the stepwise mechanism but recent density-functional

† Theoretical Studies of Organometallic Compounds, 45. Part 44: Chen, Y.; Hartmann, M.; Frenking, G. *Z. Anorg. Allg. Chem.* **2001**, *627*, 985.

(1) (a) Criegee, R. *Justus Liebigs Ann. Chem.* **1936**, *522*, 75. (b) Criegee, R.; Marchand, B.; Wannowius, H. *Justus Liebigs Ann. Chem.* **1942**, *550*, 99.

(2) For recent developments, see: (a) Döbler, C.; Mehltretter, G. M.; Sundermeier, U.; Beller, M. *J. Am. Chem. Soc.* **2000**, *122*, 10289. (b) Jonsson, S. Y.; Färnegårdh, K.; Bäckvall, J.-E. *J. Am. Chem. Soc.* **2001**, *123*, 1365.

(3) (a) Sharpless, K. B.; Teranishi, A. Y.; Bäckvall, J.-E. *J. Am. Chem. Soc.* **1977**, *99*, 3120. (b) Schröder, M.; Constable, E. C. *J. Chem. Soc., Chem. Commun.* **1982**, 734. (c) Casey, C. P. *J. Chem. Soc., Chem. Commun.* **1983**, 126. (d) Corey, E. J.; Jardine, P. D.; Virgil, S.; Yuen, P.-W.; Cornell, R. D. *J. Am. Chem. Soc.* **1989**, *111*, 9243. (e) Corey, E. J.; Noe, M. C.; Sarshar, S. *J. Am. Chem. Soc.* **1993**, *115*, 3828. (f) Corey, E. J.; Noe, M. C. *J. Am. Chem. Soc.* **1993**, *115*, 12579. (g) Sundermeyer, J. *Angew. Chem.* **1993**, *105*, 1195; *Angew. Chem., Int. Ed. Engl.* **1993**, *32*, 1144. (h) Göbel, T.; Sharpless, K. B. *Angew. Chem.* **1993**, *105*, 1417; *Angew. Chem., Int. Ed. Engl.* **1993**, *32*, 1329. (i) Becker, H.; Ho, P. T.; Kolb, H. C.; Loren, S.; Norrby, P.-O.; Sharpless, K. B. *Tetrahedron Lett.* **1994**, *35*, 7315. (j) Corey, E. J.; Sarshar, S.; Azimioara, M. D.; Newbold, R. C.; Noe, M. C. *J. Am. Chem. Soc.* **1996**, *118*, 7851. (k) Vanhessche, K. P. M.; Sharpless, K. B. *J. Org. Chem.* **1996**, *61*, 7978. (l) Corey, E. J.; Noe, M. C.; Grogan, M. J. *Tetrahedron Lett.* **1996**, *37*, 4899. (m) Rouhi, M. *Chem. Eng. News* **1997**, *75*, 23.

(4) (a) Pidun, U.; Boehme, C.; Frenking, G. *Angew. Chem.* **1996**, *108*, 3008; *Angew. Chem., Int. Ed. Engl.* **1996**, *35*, 2817. (b) Dapprich, S.; Ujaque, G.; Maseras, F.; Lledós, A.; Musaev, D. G.; Morokuma, K. *J. Am. Chem. Soc.* **1996**, *118*, 11660. (c) Torrent, M.; Deng, L.; Duran, M.; Sola, M.; Ziegler, T. *Organometallics* **1997**, *16*, 13. (d) Del Monte, A. J.; Haller, J.; Houk, K. N.; Sharpless, K. B.; Singleton, D. A.; Strassner, T.; Thomas, A. A. *J. Am. Chem. Soc.* **1997**, *119*, 9907.

(5) Metalla-2-oxetanes have been discussed as intermediates in several reactions; most of the isolated metalla-2-oxetanes known, however, are stabilized by various substituents: (a) Jørgensen, K. A.; Schiøtt, B. *Chem. Rev.* **1990**, *90*, 1483. (b) De Bruin, B.; Boerakker, M. J.; De Gelder, R.; Smits, J. M. M.; Gal, A. W. *Angew. Chem., Int. Ed. Engl.* **1999**, *38*, 219; *Angew. Chem.* **1999**, *111*, 118. (c) De Bruin, B.; Boerakker, M. J.; Verhagen, J. A. W.; De Gelder, R.; Smits, J. M. M.; Gal, A. W. *Chem. Eur. J.* **2000**, *6*, 298. (d) De Bruin, B.; Verhagen, J. A. W.; Schouten, C. H. J.; Gal, A. W.; Feichtinger, D.; Plattner, D. A. *Chem. Eur. J.* **2001**, *7*, 416. References cited therein.

(6) In recent theoretical studies, the enantioface selectivity of the Sharpless asymmetric dihydroxylation was elucidated: (a) Ujaque, G.; Maseras, F.; Lledós, A. *J. Am. Chem. Soc.* **1999**, *121*, 1317. (b) Norrby, P. A.; Rasmussen, T.; Haller, J.; Strassner, T.; Houk, K. N. *J. Am. Chem. Soc.* **1999**, *121*, 10186. (c) Moitessier, N.; Maigret, B.; Chretien, F.; Chapleur, Y. *Eur. J. Org. Chem.* **2000**, 995.

(7) (a) Gable, K. P.; Phan, T. N. *J. Am. Chem. Soc.* **1994**, *116*, 833. (b) Gable, K. P.; Juliette, J. J. J. *J. Am. Chem. Soc.* **1995**, *117*, 955. (c) Gable, K. P.; Juliette, J. J. J. *J. Am. Chem. Soc.* **1996**, *118*, 2625.

(8) (a) Herrmann, W. A.; Marz, D.; Herdtweck, E.; Schäfer, A.; Wagner, W.; Kneuper, H.-J. *Angew. Chem., Int. Ed. Engl.* **1987**, *26*, 462; *Angew. Chem.* **1987**, *99*, 462. (b) Herrmann, W. A.; Marz, D. W.; Herdtweck, E. *J. Organomet. Chem.* **1990**, *394*, 285. (c) Gable, K. P.; Phan, T. N. *J. Am. Chem. Soc.* **1993**, *115*, 3036.

(9) For reviews, see: (a) Romão, C. C.; Kühn, F. E.; Herrmann, W. A. *Chem. Rev.* **1997**, *97*, 3197. (b) Gable, K. P. *Adv. Organomet. Chem.* **1997**, *41*, 127. (c) Herrmann, W. A.; Kühn, F. E. *Acc. Chem. Res.* **1997**, *30*, 169.

10.1021/ja003733s CCC: $20.00
Published on Web 09/19/2001

Scheme 1. Postulated Mechanisms for the Reaction of OsO_4 with Olefins

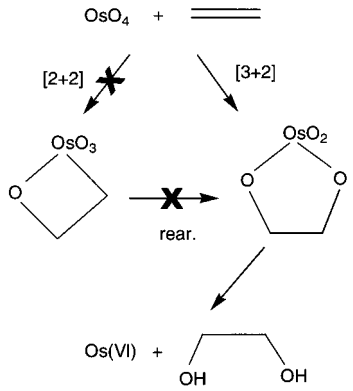

studies[10−12] again gave strong evidence for the concerted [3+2] pathway for the addition of the metal oxides $LReO_3$ (L = O^-, Cl, Cp, and Cp*) to ethylene. For the MnO_4^- addition to ethylene, the [3+2] barrier was also predicted to be lowest.[13] A recent computational study[14] supports the [2+2] addition of SO_3 to olefins but an analogous reaction for a metal oxide has not yet been reported.[15] Hence, the objective of this work is to scrutinize whether there is *any* [2+2] addition of a metal oxide across a C=C double bond.

One possible search direction is to consider activated double bonds. Ketenes are predestined for thermal [2+2] additions of organic compounds;[16] ethylene[17] and formaldehyde[18] add across the C=C double bond of the heterocumulene via the [2+2] pathway. A symmetry-allowed reaction with a supra-antarafacial attack[19] is no longer sterically hindered (Figure 1, left). The topology of the transition states (TS) has been controversially discussed and the results of a recent frontier-orbital analysis[20] are consistent with a $[2\pi_s+(2\pi_s+2\pi_s)]$ topology[21] involving the C=O moiety of ketene (Figure 1, right) rather than with the classical $[2\pi_s+2\pi_a]$ model.[21,22]

We present the first theoretical study on the addition of metal oxides to ketene. The peri-, chemo-, stereo-, and regioselectivity of the addition of OsO_4 and $LReO_3$ (L = O^-, H_3PN,[23] Me, Cp) to ketene were systematically investigated using density-functional theory (DFT). We are going to rationalize the selectivity of the metalla-analogous cycloadditions[24] by the analysis of donor−acceptor interactions in the transition states. Metal-oxide additions to diphenylketene have also been investigated experimentally;[25,26] the calculated results are discussed with respect to experimental work.

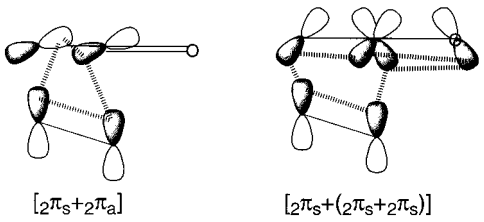

Figure 1. Suggested models for the topology of the transition state for the [2+2] addition of ethylene to ketene.

The question whether a [2+2] addition may be energetically favored over the [3+2] addition is not only of academic interest. Cycloadditions of organic compounds to ketene are widely applied in the chemical industry;[27] the production capacity of the heterocumulene is about 340 000 tons per year.[27b] Mechanistic investigations might open up new methods for an efficient activation of double bonds by readily accessible transition-metal oxides, beyond the common methods for *cis*-dihydroxylation using osmium tetraoxide and permanganate.

Methods

The geometries of the molecules and transition states (TS) were optimized at the gradient-corrected DFT level using the 3-parameter fit of exchange and correlation potentials introduced by Becke (B3LYP),[28] as implemented in Gaussian 98.[29] Relativistic small-core ECPs[30] and a (441/2111/21) valence-basis set were employed for Os and Re, while 6-31G(d) all-electron basis sets were utilized at the other atoms.[31] This basis-set combination is denoted II.[32] Vibrational frequen-

(10) Pietsch, M. A.; Russo, T. V.; Murphy, R. B.; Martin, R. L.; Rappé, A. K. *Organometallics* **1998**, *17*, 2716.

(11) Deubel, D. V.; Frenking, G. J. *J. Am. Chem. Soc.* **1999**, *121*, 2021.

(12) The activation energies for the [3+2] addition of several metal oxides to ethylene were recently predicted from thermochemical data using Marcus theory: Gisdakis, P.; Rösch, N. *J. Am. Chem. Soc.* **2001**, *123*, 697.

(13) (a) Houk, K. N.; Strassner, T. *J. Org. Chem.* **1999**, *64*, 800. (b) Strassner, T.; Busold, M. *J. Org. Chem.* **2001**, *66*, 672.

(14) Haller, J.; Beno, B. R.; Houk, K. N. *J. Am. Chem. Soc.* **1998**, *120*, 6468.

(15) [2+2] reactions of carbene complexes and related compounds with ethylene were also studied theoretically: Monteyne, K.; Ziegler, T. *Organometallics* **1998**, *17*, 5901.

(16) (a) Staudinger, H. *Die Ketene*; Enke: Stuttgart, 1912. (b) Holder, R. W. *J. Chem. Educ.* **1976**, *53*, 81. (c) Tidwell, T. T. *Acc. Chem. Res.* **1990**, *23*, 273.

(17) (a) Wang, X.; Houk, K. N. *J. Am. Chem. Soc.* **1990**, *112*, 1754 and references therein. (b) Bernardi, F.; Bottoni, A.; Robb, M. A.; Venturini, A. *J. Am. Chem. Soc.* **1990**, *112*, 2106 and references therein.

(18) (a) Lecea, B.; Arietta, A.; Roa, G.; Ugalde, J. M.; Cossio, F. P. *J. Am. Chem. Soc.* **1994**, *116*, 9613. (b) Pons, J. M.; Oblin, M.; Pommier, A.; Rajzmann, M.; Liotard, D. *J. Am. Chem. Soc.* **1997**, *119*, 3333. References cited therein.

(19) Woodward, R. B.; Hoffmann, R. *The Conservation of Orbital Symmetry*; VCH: Weinheim, 1970.

(20) Yamabe, S.; Kuwata, K.; Minato, T. *Theor. Chem. Acc.* **1999**, *102*, 139.

(21) (a) Zimmermann, H. E. In *Pericyclic Reactions*; Marchand, A. P., Lehr, R. E., Eds.; Academic Press: New York, 1977; Vol. 1. (b) Pasto, D. J. *J. Am. Chem. Soc.* **1979**, *101*, 37.

(22) Additional models for the transition state were proposed, which focus on the predominant orbital interactions rather than on the topology of the TS: (a) Ghosez, L.; O'Donnell, M. J. In *Pericyclic Reactions*; Marchand, A. P., Lehr, R. E., Eds.; Academic Press: New York, 1977; Vol. 2. (b) Yamabe, S.; Minato, T.; Osamura, Y. *Chem. Commun.* **1993**, 450.

(23) The phosphoraneiminato complexes $(R'_3PN)ReO_3$ (R′ = Et, Ph) have recently been characterized: Schlecht, S.; Deubel, D. V.; Frenking, G.; Geiseler, G.; Harms, K.; Magull, J.; Dehnicke, K. *Z. Anorg. Allg. Chem.* **1999**, *625*, 887.

(24) For a review of metalla-analogous cycloadditions, see: Frühauf, H.-W. *Chem. Rev.* **1997**, *97*, 523.

(25) (a) Herrmann, W. A.; Küsthardt, U.; Ziegler, M. L.; Zahn, T. *Angew. Chem., Int. Ed. Engl.* **1985**, *24*, 860. (b) Küsthardt, U.; Herrmann, W. A.; Ziegler, M. L.; Zahn, T.; Nuber, B. *J. Organomet. Chem.* **1986**, *311*, 163.

(26) (a) Herrmann, W. A.; Roesky, P. W.; Scherer, W.; Kleine, M. *Organometallics* **1994**, *13*, 4536. (b) Herrmann, W. A.; Küsthardt, U.; Schäfer, A.; Herdtweck, E. *Angew. Chem., Int. Ed. Engl.* **1986**, *25*, 817.

(27) (a) Wittcoff, H. A.; Reuben, B. G. *Industrial Organic Chemicals*; Wiley: New York, 1996. (b) Weissermel, K.; Arpe, H.-J. *Industrial Organic Chemistry*, 3rd ed.; Wiley-VCH: Weinheim, 1997.

(28) (a) Becke, A. D. *J. Chem. Phys.* **1993**, *98*, 5648. (b) Lee, C.; Yang, W.; Parr, R. G. *Phys. Rev. B* **1988**, *37*, 785.

(29) Frisch, M. J.; Trucks, G. W.; Schlegel, H. B.; Scuseria, G. E.; Robb, M. A.; Cheeseman, J. R.; Zakrzewski, V. G.; Montgomery, J. A.; Stratmann, R. E.; Burant, J. C.; Dapprich. S.; Milliam, J. M.; Daniels, A. D.; Kudin, K. N.; Strain, M. C.; Farkas, O.; Tomasi, J.; Barone, V.; Cossi, M.; Cammi, R.; Mennucci, B.; Pomelli, C.; Adamo, C.; Clifford, S.; Ochterski, J.; Petersson, G. A.; Ayala, P. Y.; Cui, Q.; Morokuma, K.; Malick, D. K.; Rabuck, A. D.; Raghavachari, K.; Foresman, J. B.; Cioslowski, J.; Ortiz, J. V.; Stefanov, B. B.; Liu, G.; Liashenko, A.; Piskorz, P.; Komaromi, I.; Gomberts, R.; Martin, R. L.; Fox, D. J.; Keith, T. A.; Al-Laham, M. A.; Peng, C. Y.; Nanayakkara, A.; Gonzalez, C.; Challacombe, M.; Gill, P. M. W.; Johnson, B. G.; Chen, W.; Wong, M. W.; Andres, J. L.; Head-Gordon, M.; Replogle, E. S.; Pople, J. A. *Gaussian 98*, Revision A.6; Gaussian Inc., Pittsburgh, PA, 1998.

(30) Hay, P. J.; Wadt, W. R. *J. Chem. Phys.* **1985**, *82*, 299.

(31) (a) Binkley, J. S.; Pople, J. A.; Hehre, W. J. *J. Am. Chem. Soc.* **1980**, *102*, 939. (b) Hehre, W. J.; Ditchfield, R.; Pople, J. A. *J. Chem. Phys.* **1972**, *56*, 2257.

cies and zero-point energies (ZPE) were also calculated at B3LYP/II. All structures reported here are either minima (NIMAG = 0) or transition states (NIMAG = 1) on the potential-energy surfaces. The ZPE contributions are unscaled. Starting with the TS geometries, calculations of the Intrinsic Reaction Coordinate (IRC)[33] were carried out to determine the respective reactants and products. Improved total energies were calculated at the B3LYP level using the same ECP and valence-basis set at the metals, but totally uncontracted and augmented with one set of f-type polarization functions,[34] together with 6-31+G(d) basis sets at the other atoms.[35] This is our basis set III+.[11] Unless otherwise mentioned, energies reported refer to the B3LYP/III+//B3LYP/II level including ZPE corrections at the B3LYP/II level and optimized geometries refer to the B3LYP/II level. These methods were proved to give results in good agreement with experimental data.[11,36] For the calculation of atomic partial charges, the NPA method[37] was employed. Donor−acceptor interactions in the transition states were examined using Charge Decomposition Analysis (CDA).[38] The CDA calculations were performed with the program CDA 2.1.[39] Selected molecules were optimized at the gradient-corrected DFT level using the exchange functional of Becke[40] and the correlation functional of Perdew[41] (BP86). Relativistic effects were considered using the zero-order regular approximation (ZORA).[42] Uncontracted Slater-type orbitals (STOs) were used as basis functions for the SCF calculations.[43] The basis functions at the metals have triple-ζ quality, augmented with a set of 6p functions. The basis set at the other atoms has double-ζ quality, augmented with a set of d-type polarization functions. The $(1s)^2$ core electrons of C, N, and O, the $(1s2s2p)^{10}$ core electrons of P, and the $(1s2s2p3s3p3d4s4p4d)^{46}$ inner shells of the metals were treated within the frozen-core approximation.[44] An auxiliary basis set of s, p, d, f, and g STOs was utilized to fit the molecular densities and to represent the Coulomb and exchange potentials in each SCF cycle.[45] This basis-set combination is denoted III∼. The calculations at the BP86/III∼ level were carried out using the ADF 2000 program package.[46]

Results

Metal-Oxide Additions to Ethylene. The optimized geometries of the reactants are shown in Figure 2. We briefly report

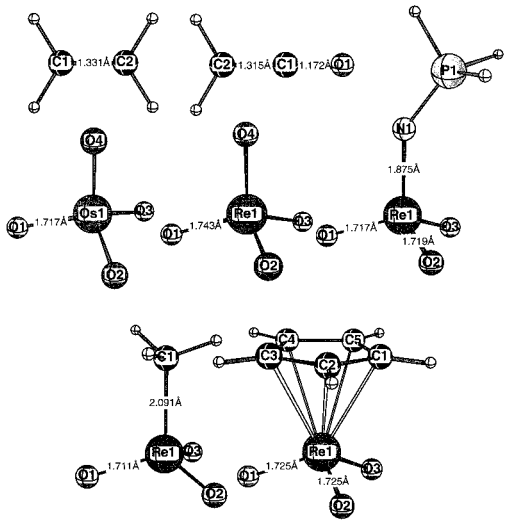

Figure 2. Optimized geometries of the reactants C_2H_4, H_2CCO, OsO_4, ReO_4^-, $(H_3PN)ReO_3$, $MeReO_3$, and $CpReO_3$.

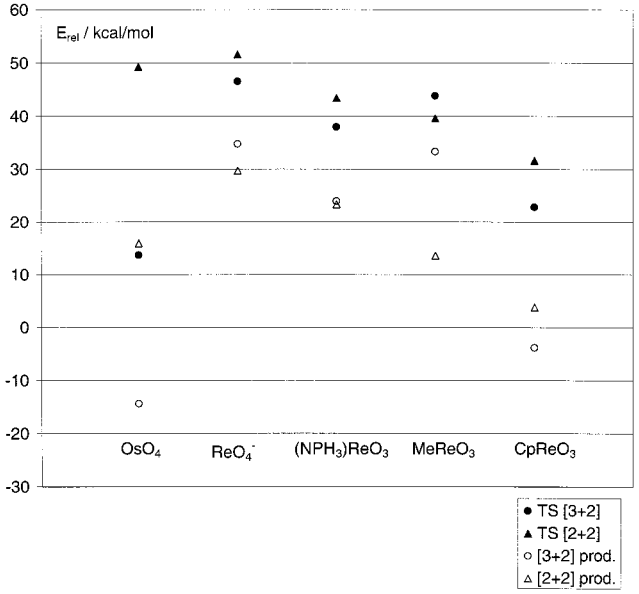

Figure 3. Calculated thermodynamic and kinetic reaction profile for the addition of LMO_3 to ethylene. If there are cis and trans isomers, only the most stable configuration is shown.

new results for the [3+2] and [2+2] reactions of the metal oxides $LReO_3$ (L = H_3PN, Me) with ethylene, which were not addressed in our previous study.[11] We focus on the activation and reaction energies only, which are reported in Table 1 and visualized in Figure 3. As for OsO_4, ReO_4^-, and $CpReO_3$,[11] a [3+2] periselectivity of the addition of $(H_3PN)ReO_3$ to ethylene was found, however, with a high barrier (37.9 kcal/mol) and reaction energy (23.9 kcal/mol). Although the activation energies for the $MeReO_3$ addition are also calculated to be large, the energy profile is very interesting: $MeReO_3$ is the first metal oxide with a calculated [2+2] barrier (39.6 kcal/mol) lower than the [3+2] barrier (43.8 kcal/mol), arising from the 33.3 kcal/mol endothermic formation of the metalla-2,5-dioxolane ([3+2] product). Note that the [3+2] addition of $CpReO_3$ is exothermic by −3.9 kcal/mol.[11]

Metal-Oxide Additions to Ketene. Metal-oxide additions to ketene might follow a variety of reaction paths. Besides periselectivity ([3+2] versus [2+2]) and stereoselectivity (cis and trans isomers for the [2+2] transition states and products), there is also a chemoselectivity (addition across the C=C or

(32) Frenking, G.; Antes, I.; Böhme, M.; Dapprich, S.; Ehlers, A. W.; Jonas, V.; Neuhaus, A.; Otto, M.; Stegmann, R.; Veldkamp, A.; Vyboishchikov, S. F. *Reviews in Computational Chemistry*; Lipkowitz, K. B., Boyd, D. B., Eds.; VCH: New York, 1996; Vol. 8, p 63.
(33) Fukui, K. *Acc. Chem. Res.* **1981**, *14*, 363.
(34) Ehlers, A. W.; Böhme, M.; Dapprich, S.; Gobbi, A.; Höllwarth, A.; Jonas, V.; Köhler, K. F.; Stegmann, R.; Veldkamp A.; Frenking, G. *Chem. Phys. Lett.* **1993**, *208*, 111.
(35) Clark, T.; Chandrasekhar, J.; Spitznagel, G. W.; Schleyer, P. v. R. *J. Comput. Chem.* **1983**, *4*, 294.
(36) Gisdakis, P.; Antonczak, S.; Rösch, N. *Organometallics* **1999**, *18*, 5044.
(37) Reed, A. E.; Curtiss, L. A.; Weinhold, F. *Chem. Rev.* **1988**, *88*, 899.
(38) Dapprich, S.; Frenking, G. *J. Phys. Chem.* **1995**, *99*, 9352.
(39) *CDA 2.1*; Dapprich, S.; Frenking, G., Marburg, 1994. The program is available via ftp.chemie.uni-marburg.de/pub/cda.
(40) Becke, A. D. *Phys. Rev. A* **1988**, *38*, 3098.
(41) Perdew, J. P. *Phys. Rev. B* **1986**, *33*, 8822.
(42) (a) Chang, C.; Pelissier, M.; Durand, P. *Phys. Scr.* **1986**, *34*, 394. (b) Heully, J.-L.; Lindgren, I.; Lindroth, E.; Lundquist, S.; Martensson-Pendrill, A. M. *J. Phys. B* **1986**, *19*, 2799. (c) Van Lenthe, E.; Baerends, E. J.; Snijders, J. G. *J. Chem. Phys.* **1993**, *99*, 4597. (d) Van Lenthe, E.; Baerends, E. J.; Snijders, J. G. *J. Chem. Phys.* **1996**, *105*, 6505. (e) Van Lenthe, E.; Van Leeuven, R.; Baerends, E. J.; Snijders, J. G. *Int. J. Quantum Chem.* **1996**, *57*, 281. (f) Van Lenthe, E.; Ehlers, A. E.; Baerends, E. J. *J. Chem. Phys.* **1999**, *110*, 8943.
(43) Snijders, J. G.; Baerends, E. J.; Vernooijs, P. *At. Data Nucl. Tables* **1982**, *26*, 483.
(44) Baerends, E. J.; Ellis, D. E.; Ros, P. *Chem. Phys.* **1973**, *2*, 41.
(45) Krijn, J. G.; Baerends, E. J. *Fit Functions in the HFS-Method*; Internal Report (in Dutch); Vrije Universiteit Amsterdam: The Netherlands, 1984.
(46) (a) Fonseca Guerra, C.; Snijders, J. G.; Te Felde, G.; Baerends, E. J. *Theor. Chem. Acc.* **1998**, *99*, 391. (b) Bickelhaupt, F. M.; Baerends, E. J. *Rev. Comput. Chem.* **2000**, *15*, 1. (c) Te Velde, G.; Bickelhaupt, F. M.; Baerends, E. J.; Fonseca Guerra, C.; Van Gisbergen, S. J. A.; Snijders, J. G.; Ziegler, T. *J. Comput. Chem.* **2001**, *22*, 931.

Table 1. Calculated Relative Energies (B3LYP/III+//B3LYP/II) [kcal/mol] for the [3+2] and [2+2] Addition of LMO_3 (M = Os, L = O; M = Re, L = O^-, H_3PN, CH_3, Cp, Cp*) Across the C=C Bond of Ethylene and Ketene[d]

					TS [2+2] C=C		[2+2] C=C product		TS rearrangement	
LMO_3	C=C	LMO_3 + C=C	TS [3+2]	[3+2] product	cis	trans	cis	trans	cis	trans
OsO_4	ethylene[a]	0.0 (0.0)	11.8 (13.7)	−19.1 (−14.4)	47.9 (49.2)	*b*	12.7 (15.9)	*b*	45.4 (47.6)	*b*
ReO_4^-	ethylene[a]	0.0 (0.0)	44.8 (46.5)	30.8 (34.7)	50.6 (51.6)	*b*	27.2 (29.7)	*b*	108.1 (109.7)	*b*
$(H_3PN)ReO_3$	ethylene	0.0 (0.0)	35.9 (37.9)	19.6 (23.9)	41.7 (43.4)	44.5 (46.0)	20.3 (23.3)	9.2 (13.0)	66.6 (68.8)	64.8 (67.0)
CH_3ReO_3	ethylene	0.0 (0.0)	41.9 (43.8)	29.6 (33.3)	37.5 (39.6)	47.7 (49.3)	10.9 (14.7)	10.1 (13.6)	66.9 (69.2)	62.7 (65.3)
$CpReO_3$	ethylene[a]	0.0 (0.0)	20.7 (22.8)	−8.7 (−3.9)	29.9 (31.6)	37.8 (39.2)	4.7 (7.8)	0.9 (3.8)	58.3 (60.2)	60.0 (62.2)
Cp^*ReO_3	ethylene[a]	0.0 (0.0)	23.0 (25.1)		41.5[c]	40.3[c]				
OsO_4	ketene	0.0 (0.0)	18.1 (19.5)	−31.7 (−26.9)	24.6 (26.4)	*b*	−2.5 (0.8)	*b*	26.5 (28.6)	*b*
ReO_4^-	ketene	0.0 (0.0)	28.4 (30.5)	−0.1 (4.4)	12.4 (14.3)	*b*	−8.3 (−5.1)	*b*	55.5 (57.8)	*b*
$(H_3PN)ReO_3$	ketene	0.0 (0.0)	36.9 (38.4)	2.0 (6.6)	23.0 (24.9)	21.1 (22.9)	−0.4 (2.8)	−10.9 (−7.0)	45.7 (48.0)	43.2 (45.8)
CH_3ReO_3	ketene	0.0 (0.0)	44.5 (45.8)	16.3 (20.3)	20.2 (22.4)	23.6 (25.3)	−6.3 (−2.3)	−9.9 (−6.1)	46.8 (49.0)	42.6 (45.5)
$CpReO_3$	ketene	0.0 (0.0)	24.8 (26.3)	−29.2 (−24.0)	9.1 (10.8)	11.8 (13.0)	−14.0 (−10.8)	−20.2 (−17.0)	35.4 (38.0)	36.9 (39.7)
Cp^*ReO_3	ketene	0.0	26.7[c]		25.3[c]	20.8[c]				

[a] Relative energies taken from the following: Deubel, D. V.; Frenking, G. *J. Am. Chem. Soc.* **1999**, *121*, 2021. [b] No cis/ trans isomers. [c] Starting geometry taken from the analogous Cp system. Only internal Cp* coordinates and Re−C(Cp*) distances were optimized. [d] ZPE (B3LYP/II)-corrected relative energies are given in parentheses.

Scheme 2. Reaction Paths for the Addition of Metal Oxides LMO_3 to Ketene, Represented by Their Transition States

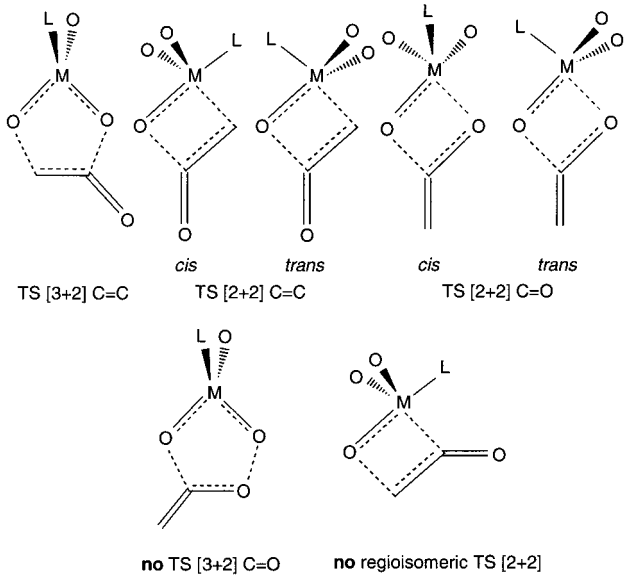

C=O moiety). The [3+2] addition across the C=O bond is expected to be unfavored because a metalla-2,3,5-trioxolane containing an endocyclic O−O bond would be formed. Indeed, we could not localize a transition state for the [3+2] addition of $LReO_3$ (L = H_3PN, Me) across the C=O moiety on the potential-energy surface and dropped considering this pathway (Scheme 2). Furthermore, a potential regioselectivity of the [2+2] pathways was not systematically taken into account because a transition state for the formation of a metalla-2-oxetane-4-one instead of the 2-oxetane-3-one could also not be located on the potential-energy surface. The remaining pathways, represented by their transition states, are shown in Scheme 2; the notations cis and trans refer to the position of the ligand L to the metal−carbon or metal−oxygen bond, respectively, that is newly formed. The rearrangement of the [3+2] C=C and [2+2] C=C products was also studied.

Figure 4 shows the theoretically predicted geometries of the transition states and products for the reaction of $(H_3PN)ReO_3$ with ketene.[47] The corresponding structures for the addition of the other metal oxides are very similar; the most important geometrical parameters of the transition states are listed in Table 2. A thorough discussion of the structures for the additions to ethylene was given in our previous study;[11] here, we only focus on the differences between the reactions with the two substrates. In contrast to the metalla-2,5-dioxolanes, the metalla-2,5-dioxolane-3-ones are planar. This is due to conjugation with the exocyclic C=O bond, which is also indicated by the short C1−O3 distances (Figure 4). The four-membered rings have a planar geometry, too. However, the transition states for the additions across the C=C moiety are nonplanar since the HOMO and LUMO of ketene are π orbitals with perpendicular orientations.[48] The TS geometries for the [3+2] additions of the rhenium oxides indicate strongly asynchronous reactions; the bond to the central carbon of ketene is formed first. The calculation of the Intrinsic Reaction Coordinate (IRC)[33] shows that the cycloadditions are concerted. Both the transition states and the products for the [2+2] additions across the C=O moiety are planar because the HOMO-1 (π-C=O orbital) and the LUMO of ketene are involved and both orbitals have the same nodal plane.[48] Structural differences between the cis and trans configurations of the [2+2] transition states and products, respectively, can be understood with the thermodynamic and kinetic trans influence. Considering the [2+2]-C=C TSs for $(H_3PN)ReO_3$, for instance, the Re−C2 distance in the cis isomer is longer than that in the trans isomer because, in the latter TS, the H_3PN ligand is situated trans to the bond being newly formed and, in the former isomer, a stronger oxo ligand is in trans position to the new Re−C2 bond.

The calculated activation and reaction energies are listed in Tables 1 and 3 and visualized in Figure 5. In general, the lowest activation barriers are between 10 and 20 kcal/mol and the favored reactions are exothermic, indicating that cycloadditions to ketene are experimentally accessible for each of the investigated metal oxides. The theoretically predicted peri- and chemoselectivities are intriguing: For OsO_4, the [3+2] pathway is thermodynamically and kinetically favored. In contrast, ReO_4^- and $(H_3PN)ReO_3$ prefer [2+2] pathways: The activation barrier for the C=O addition is lower than that for the C=C addition while the energies of the products are reverse. $MeReO_3$ favors the [2+2] addition across the C=C moiety, both thermodynamically and kinetically. For $CpReO_3$, the [2+2] C=C activation barrier is also calculated to be lowest but the [3+2] product is

(47) Complexes with phosphoraneiminato ligands show an anomeric effect, which has recently been discussed for molybdenum-oxo-peroxo compounds with R_3PO ligands: Deubel, D. V.; Sundermeyer, J.; Frenking, G. *Inorg. Chem.* **2000**, *39*, 2314. For example, the Re−O1 bond length in $(H_3PN)ReO_3$ is slightly shorter than the other Re−O distances of the molecule (Figure 2).

(48) Fleming, I. *Frontier Orbitals and Organic Chemical Reactions*; Wiley: New York, 1976.

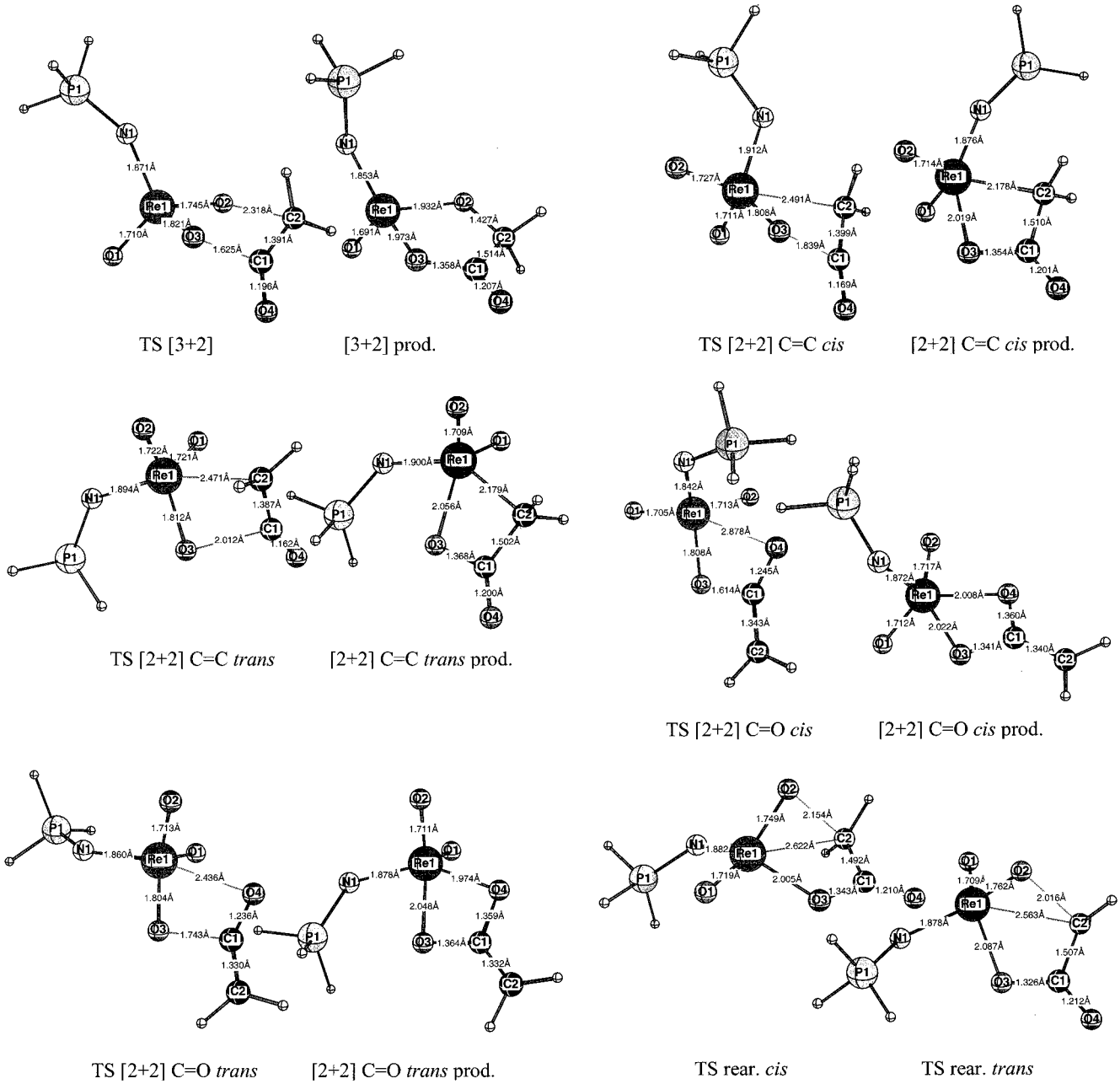

Figure 4. Optimized geometries of the transition states and products for the reaction of $(H_3PN)ReO_3$ with ketene.

Table 2. Calculated Distances [Å] in the Transition States for the Addition of Metal Oxides to Ketene (B3LYP/II)

	TS [3+2]		TS [2+2] C=C *cis*		TS [2+2] C=C *trans*		TS [2+2] C=O *cis*		TS [2+2] C=O *trans*	
LMO_3	O−C(H_2)	O−C(O)	M−C	O−C(O)	M−C	O−C(O)	M−O	O−C(CH_2)	M−O	O−C(CH_2)
OsO_4	2.041	2.091	2.450	1.906	*a*	*a*	2.879	1.515	*a*	*a*
ReO_4^-	2.251	1.439	3.198	1.556	*a*	*a*	2.869	1.579	*a*	*a*
$(H_3PN)ReO_3$	2.318	1.625	2.491	1.839	2.471	2.011	2.878	1.614	2.436	1.743
CH_3ReO_3	2.349	1.525	2.444	1.972	2.502	1.906	2.428	1.795	*b*	*b*
$CpReO_3$	2.213	1.833	2.472	1.969	2.467	1.909	2.456	1.823	2.442	1.643

[a] No cis/trans isomers. [b] Geometry optimization yielded the cis isomer only.

the most stable metallacycle. In general, the differences between the [2+2] barriers are small for all five metal oxides.

The remarkable deviations of the calculated energy profile for the additions of $MeReO_3$ to ketene from the corresponding $CpReO_3$ profile (Figure 5) can be rationalized considering the Re−C(Cp) distances in the optimized structures (Table 4). The role of the Cp ligand as a stereoelectronic mediator adopting η^5, η^3, and η^1 bond modes was already pointed out for the $CpReO_3$ addition to ethylene.[11] This unique property can be quantitatively evaluated by a comparison of the energy profiles for the two metal oxides since Me is an appropriate model for η^1-Cp. In all [2+2] transition states and products of the $CpReO_3$ additions to ketene, the Cp ligand adopts a η^1 coordination. The calculated [2+2] reaction barriers and energies shown in Figure 5 indicate an activation of η^5-$CpReO_3$ by ca. 10 kcal/mol. The [3+2] product is stabilized by 44.3 kcal/mol due to the η^3 bond mode in conjunction with significantly shortened Re−C(Cp) distances (Table 4).

Table 3. Calculated Relative Energies (B3LYP/III+//B3LYP/II) [kcal/mol] for the [2+2] Addition of LMO_3 (M = Os, L = O; M = Re, L = O^-, H_3PN, CH_3, Cp, Cp*) Across the C=O Moiety of Ketene[d]

LMO_3	LMO_3 + ketene	TS [2+2] C=O cis	TS [2+2] C=O trans	[2+2] C=O product cis	[2+2] C=O product trans
OsO_4	0.0 (0.0)	32.7 (33.6)	*a*	9.4 (12.6)	*a*
ReO_4^-	0.0 (0.0)	9.6 (11.2)	*a*	−2.3 (0.8)	*a*
(H_3PN)-ReO_3	0.0 (0.0)	14.1 (16.1)	26.6 (27.8)	5.9 (9.1)	0.0 (3.6)
CH_3ReO_3	0.0 (0.0)	23.3 (24.6)	*b*	0.5 (4.3)	*b*
$CpReO_3$	0.0 (0.0)	12.9 (13.8)	22.1 (22.6)	−5.3 (−2.5)	−8.9 (−5.9)
Cp^*ReO_3	0.0	24.3[c]	23.5[c]		

[a] No cis/trans isomers. [b] Geometry optimization yielded the cis isomer only. [c] Starting geometry taken from the analogous Cp system. Only internal Cp* coordinates and Re−C(Cp*) distances were optimized. [d] ZPE (B3LYP/II)-corrected relative energies are given in parentheses.

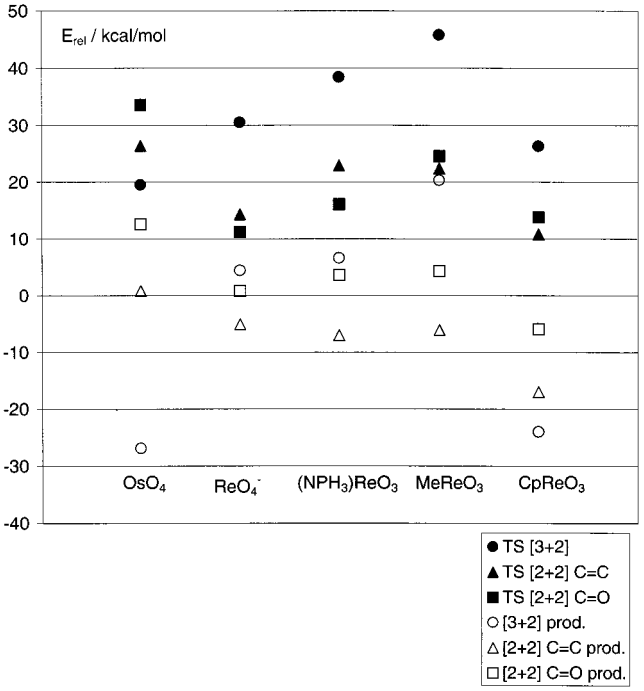

Figure 5. Calculated thermodynamic and kinetic reaction profile for the addition of LMO_3 to ketene. If there are cis and trans isomers, only the most stable configuration is shown.

Table 4. Calculated Re−C(Cp) Distances [Å] in the Reactant, in the Transition States, and in the Products of the $CpReO_3$ Addition to Ketene (B3LYP/II) and Coordination Mode η^a

molecule/TS	Re−C3	Re−C4	Re−C5	Re−C6	Re−C7	η^a
$CpReO_3$	2.473	2.488	2.481	2.481	2.488	5
TS [3+2]	2.371	2.425	2.552	2.562	2.443	3
[3+2] prod.	2.209	2.294	2.524	2.522	2.280	3
TS [2+2] C=C cis	2.188	2.891	3.727	3.798	3.024	1
TS [2+2] C=C trans	2.172	2.932	3.724	3.734	2.951	1
[2+2] C=C cis prod.	2.174	2.890	3.786	3.875	3.077	1
[2+2] C=C trans prod.	2.172	2.920	3.767	3.807	2.998	1
TS rear. cis	2.327	2.389	2.509	2.599	2.489	2
TS rear. trans	2.306	2.379	2.564	2.690	2.539	2
TS [2+2] C=O cis	2.148	2.767	3.594	3.715	2.996	1
TS [2+2] C=O trans	2.121	2.796	3.500	2.502	2.801	1
[2+2] C=O cis prod.	2.140	3.015	3.777	3.674	2.818	1
[2+2] C=O trans prod.	2.158	2.942	3.809	3.837	3.001	1

[a] Criterion: All Cp-carbon atoms with a Re−C distance smaller than the shortest Re−C distance + 0.15 Å were considered.

The predicted stereoselectivity of the [2+2] additions is very interesting: In all metalla-2-oxetane-3-ones ([2+2] C=C products) and 3-methylene-metalla-2,4-dioxetanes ([2+2] C=O products), the trans configuration is considerably more stable than the cis isomer. However, in most cases, the cis pathway is kinetically favored (Tables 1 and 3).[49] This puzzling result is elucidated as follows. Calculated NPA partial charges *q*(O) at the oxygen atoms of the rhenium oxides $LReO_3$ illuminate that the donor strength of L increases is the order η^5-Cp < Me ≈ η^1-Cp < H_3PN < O^- (Table 5). The stability of the [2+2] C=C products with a comparably weak L ≠ O^- ligand in the trans position to the $CH_2(CO)^-$ moiety of the metallacycle indicates that the $CH_2(CO)^-$ moiety is more strongly bound to the metal than the carboxylate moiety with its delocalized charge. In the corresponding transition states, however, the carboxylate moiety competes with the Re−C2 bond, which is only partially formed (Figure 4). Therefore, the stronger oxo ligand prefers the position trans to the partial Re−C2 bond in the transition states.

Table 5. Frontier-Orbital Energies ϵ [au] and Atomic Partial Charges *q* [au] of the Metal Oxides LMO_3, Ethylene, and Ketene

molecule	PG	ϵ (HOMO)		ϵ (LUMO)		*q*(M)	*q*(O)	*q*(C1)	*q*(C2)
OsO_4	T_d	t_1	−0.370	*e*	−0.167	2.24	−0.56		
ReO_4^-	T_d	t_1	−0.108	*e*	0.131	2.18	−0.80		
(H_3PN)-ReO_3	C_s	*a*″ [a]	−0.300	*a*″	−0.082	2.13	−0.65		
CH_3ReO_3	C_{3v}	*a*	−0.339	*e*	−0.121	2.04	−0.61		
$CpReO_3$	C_s	*a*″ [a]	−0.300	*a*″	−0.079	1.92	−0.58		
ethylene	D_{2h}	b_{3u}	−0.267	b_{2g}	0.019			−0.43	−0.43
ketene	C_{2v}	b_1	−0.240	b_2	−0.036		−0.45	0.70	−0.79
		b_2[b]	−0.403						

[a] Instead of HOMO, HOMO-2 was identified as the dominant orbital of the donor−acceptor interaction. [b] HOMO-1.

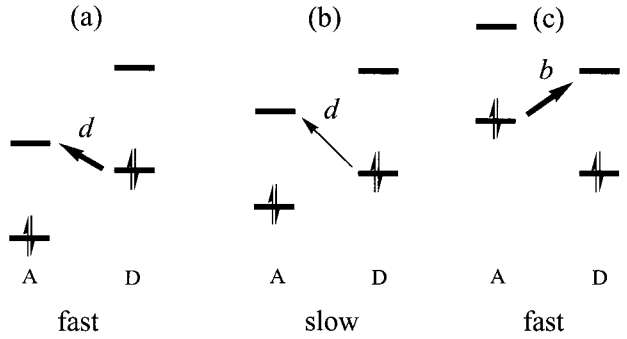

Figure 6. Cycloadditions of organic molecules: Relation between reactivity and the frontier-orbital interactions donation *d* and back-donation *b* between the fragments donor (D) and acceptor (A).

Discussion

Donor−Acceptor Interactions in the Transition States. The relative activation barriers of cycloadditions, such as Diels−Alder reactions, can be understood using the concept of frontier-orbital analysis.[48,50,51] One reactant is arbitrarily denoted *donor*, D; the other reactant is denoted *acceptor*, A. Assume that the acceptor is activated by electron-withdrawing substituents decreasing the frontier-orbital levels of A. Then, electron donation *d* from the D HOMO to the A LUMO will provide the predominant orbital interaction and the reaction is expected to be fast (Figure 6a). A rise of the orbital levels of A relative to D leads to a weaker donation and a smaller reactivity (Figure 6b). However, a further relative increase of the frontier orbitals

(49) A mutual rearrangement of the cis and trans products was not investigated in this study.

(50) Fukui, K. *Theory of Orientation and Stereoselection*; Springer: Berlin, 1970.

(51) (a) Houk, K. N. *J. Am. Chem. Soc.* **1973**, *95*, 4092. (b) Houk, K. N. *Acc. Chem. Res.* **1975**, *8*, 361. (c) Houk, K. N. *Top. Curr. Chem. Soc.* **1979**, *79*, 1. (d) Sauer, J.; Schubert, R. *Angew. Chem., Int. Ed.* **1980**, *19*, 779.

Table 6. CDA Results of the Transition States [Donation *d* ($XY \rightarrow LMO_3$), Backdonation *b* ($XY \leftarrow LMO_3$), Ratio *d*/*b*, Repulsive Polarization *r* ($XY \leftrightarrow LMO_3$), and Rest Term Δ]

TS	LMO_3	XY	cis/trans	*d*	*b*	*d*/*b*	*r*	Δ
[3+2]	OsO_4	ethylene		0.192	0.153	1.25	−0.360	0.000
	ReO_4^-			0.191	0.275	0.69	−0.636	0.057
	$(NPH_3)ReO_3$			0.213	0.256	0.83	−0.648	0.004
	$MeReO_3$			0.218	0.262	0.83	−0.669	0.006
	$CpReO_3$			0.207	0.216	0.96	−0.507	0.000
[2+2]	OsO_4	ethylene		0.303	0.100	3.03	−0.319	0.134
	ReO_4^-			0.258	0.187	1.38	−0.441	0.132
	$(NPH_3)ReO_3$		cis	0.344	0.147	2.34	−0.405	0.111
	$(NPH_3)ReO_3$		trans	0.322	0.126	2.56	−0.386	0.137
	$MeReO_3$		cis	0.349	0.123	2.84	−0.370	0.110
	$MeReO_3$		trans	0.308	0.098	3.14	−0.322	0.096
	$CpReO_3$		cis	0.353	0.123	2.87	−0.374	0.107
	$CpReO_3$		trans	−0.200	0.054	−3.70	0.016	−0.204
[3+2]	OsO_4	ketene		0.191	0.160	1.19	−0.361	0.001
	ReO_4^-			0.163	0.565	0.29	−0.682	0.026
	$(NPH_3)ReO_3$			0.165	0.343	0.48	−0.566	0.014
	$MeReO_3$			0.152	0.420	0.36	−0.605	0.022
	$CpReO_3$			0.178	0.247	0.72	−0.449	0.005
[2+2] C═C	OsO_4	ketene		0.352	0.166	2.37	−0.428	0.063
	ReO_4^-			0.240	0.382	0.63	−0.564	0.045
	$(NPH_3)ReO_3$		cis	0.376	0.201	1.87	−0.478	0.048
	$(NPH_3)ReO_3$		trans	0.360	0.163	2.21	−0.396	0.039
	$MeReO_3$		cis	0.389	0.161	2.42	−0.430	0.041
	$MeReO_3$		trans	0.350	0.180	1.94	−0.429	0.051
	$CpReO_3$		cis	0.394	0.171	2.30	−0.432	0.038
	$CpReO_3$		trans	0.362	0.179	2.02	−0.438	0.054
[2+2] C═O	OsO_4	ketene		0.147	0.345	0.43	−0.533	0.055
	ReO_4^-			0.156	0.329	0.47	−0.472	0.045
	$(NPH_3)ReO_3$		cis	0.363	0.474	0.77	−0.548	0.015
	$(NPH_3)ReO_3$		trans	0.275	0.220	1.25	−0.400	0.042
	$MeReO_3$		cis	0.299	0.213	1.40	−0.377	0.027
	$CpReO_3$		cis	0.294	0.202	1.46	−0.364	0.025
	$CpReO_3$		trans	0.283	0.250	1.13	−0.468	0.060

of A might reverse the orbital interactions and cause back-donation *b* from the A HOMO to the D LUMO to be more important than *d*, which can result in a higher reactivity (Figure 6c).

For cycloadditions involving transition-metal compounds, however, an analysis solely based on HOMO and LUMO of the reactants is incomplete since several frontier orbitals of the metal compound might contribute to the predominant orbital interactions.[11] An improved concept is required. There is a method giving insight into the relative importance of donation and back-donation in the transition states for cycloadditions involving transition-metal compounds: Charge Decomposition Analysis (CDA).[38] The Kohn−Sham orbitals of the TS are expressed as a linear combination of the orbitals of the fragments donor and acceptor. The orbital interactions are divided into the mixing of the occupied MOs of the donor and the vacant orbitals of the acceptor (donation *d*), the mixing of the vacant MOs of the donor and the occupied orbitals of the acceptor (back-donation *b*), and the mixing of the occupied MOs between both fragments (repulsive polarization *r*). A fourth contribution denoted rest term Δ gives the mixing among the unoccupied MOs of both fragments. The Δ term will be approximately zero if a discussion of the transition states in terms of donor−acceptor interactions is permissible and the reactions are symmetry-allowed. Very recently, CDA has successfully been utilized to clarify the electronic character of oxygen-transfer reactions with coarctate transition states and as a tool for the design of catalysts for olefin epoxidation.[52]

We analyzed the transition states for the metal-oxide additions using CDA; the results are listed in Table 6. Ethylene and ketene, respectively, are defined as donor and LMO_3 is defined as acceptor. The most important contributions to *d* and *b* in the TS for the [2+2] addition of $(H_3PN)ReO_3$ across the C═C bond of ketene are visualized in Figure 7. Our discussion focuses on the plot of the activation energies E_a versus ln(*d*/*b*) given in Figure 8.[53] The analysis reveals that the barriers for the [3+2] additions to ethylene well correlate with ln(*d*/*b*) (**I**): The larger *d*, the more reactive is the metal oxide. The [3+2] additions to ketene can be rationalized in a similar manner (**II**). There is one exception (**III**): Despite the small *d*/*b* value, the activation barrier for perrhenate is comparably low. This result might be explained by a reverse reactivity (Figure 6c).

The high values of the rest term Δ for the [2+2] additions to ethylene (Table 6) indicate that these reactions are symmetry-forbidden. The CDA results (**IV**) have to be interpreted with caution because the analysis yields an unphysical negative *d* value ($CpReO_3$, trans, Table 6). In contrast, the [2+2] reactions of LMO_3 with ketene are symmetry-allowed and the rest terms Δ are close to 0 (Table 6). All [2+2] additions of the five metal oxides across the C═C bond of ketene have about the same *d*/*b* values and about the same activation energies (**V**). ReO_4^- is again an exception (**VI**): The small *d*/*b* value indicates that a nucleophilic attack of perrhenate dominates at the beginning of the concerted cycloaddition. This nucleophilic attack is also reflected by the short O−C(O) distance and the long M−C distance in the transition structure of the ReO_4^- addition to ketene (Table 2).

(52) (a) Deubel, D. V.; Sundermeyer, J.; Frenking, G. *J. Am. Chem. Soc.* **2000**, *122*, 10101. (b) Deubel, D. V.; Frenking, G.; Senn, H. M.; Sundermeyer, J. *Chem. Commun.* **2000**, 2469. (c) Deubel, D. V.; Sundermeyer, J.; Frenking, G. *Eur. J. Inorg. Chem.* **2001**, 1819. (d) Deubel, D. V. *J. Org. Chem.* **2001**, *66*, 3790.

(53) We chose a plot of E_a versus ln(*d*/*b*) instead of *d*/*b* since the definition of the donor and the acceptor is arbitrary.

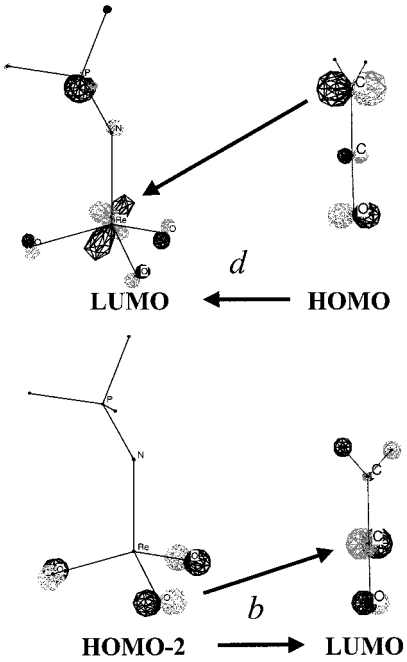

Figure 7. Predominant contributions to donation *d* and back-donation *b* in the transition state for the [2+2] addition of $(H_3PN)ReO_3$ across the C═C moiety of ketene, according to CDA.

The [2+2] reactions across the C═O moiety have activation barriers similar to the corresponding C═C additions but smaller *d* values (**VII**). These smaller *d* values arise from the fact that the energy level of the π C═O orbital (HOMO-1) is lower than that of the π C═C (HOMO) level (Table 5). Beside ReO_4^-, there are two additional exceptions (**VIII**). According to the partial charges *q*(O) at the oxygen atoms of the free metal oxides (Table 5), O^- is the strongest ligand L and H_3PN is the second strongest ligand. While the trans TS of the $(H_3PN)ReO_3$ reaction belongs to section **VII**, the cis configuration belongs to **VIII**. In the latter isomer, an early formation of the metal−O4 bond is prevented by the strong oxo ligand in the trans position (Figure 4). Surprisingly, the [2+2] addition of OsO_4 across the C═O bond also belongs to section **VIII** although osmium tetraoxide has the smallest O-nucleophilicity of the five metal oxides (Table 5). Despite the high positive partial charge at the metal, Os(VIII) is apparently less electrophilic than Re(VII).

Comparison to Experimental Studies. Current experimental work is focusing on the addition of $(R'_3PN)ReO_3$ ($R' = Me$) to diphenylketene R_2CCO ($R = Ph$).[54] Although we have intended to elucidate metal-oxide additions to ketene rather than to diphenylketene in this computational study, a comparison to those experimental results is interesting. ^{13}C NMR chemical shifts indicate that the reaction of $(Me_3PN)ReO_3$ with diphenylketene gives the metalla-2-oxetane-3-one ([2+2] C═C product),[54] which is the metallacycle predicted to be most stable ($R = H$, $R' = H$). However, the calculated activation energy for the C═O addition is lower by 6.8 kcal/mol than the C═C barrier ($R = H$, $R' = H$, Figure 5). We would like to point out that R'_3PN ($R' = H$) is a good computational model for $R' =$ Me; the calculated activation barriers for $R' = H$ and $'$ Me are almost equal.[55] The effects of the phenyl substituents and solvation might therefore influence the chemoselectivity of the [2+2] addition. In the pioneering experimental work,[25] the reaction of Cp^*ReO_3 with diphenylketene was reported, yielding the metalla-2,5-dioxolane-3-one. The [3+2] product was characterized by X-ray analysis, leaving no doubt on the experimental result.[25] Although we predict the [3+2] product to be thermodynamically favored in the reaction of $CpReO_3$ with ketene, the calculated [2+2] C═C activation barrier is smaller by 15.5 kcal/mol than the [3+2] activation energy (Figure 5). An interconversion of the [3+2] and [2+2] C═C products can be ruled out due to very high relative energies of the transition states for rearrangement (Table 1). To reveal the difference between Cp and Cp*, we have investigated the [3+2] and [2+2] transition states for the Cp^*ReO_3 addition to ketene by partial optimization (Tables 1 and 3). The activation energies for the [2+2] additions of Cp^*ReO_3 are much higher than those for $CpReO_3$. The Cp* ligand apparently prefers η^5 and η^3 modes rather than η^1 coordination. In contrast, the calculated [3+2] barrier increases only slightly using the Cp* model. For all five TS, the predicted activation barriers lie between 20.8 and 26.7 kcal/mol. The calculated [3+2] activation energy of 26.7 kcal/mol does not agree with the fact that Cp^*ReO_3 reacts with diphenylketene at room temperature.[25]

How can we explain the puzzling deviation between the selectivities found experimentally and predicted theoretically? Consider the calculated transition-state geometries (Table 2, Figure 4), some of which already reflect a nucleophilic attack of the oxo functionality of the metal oxide at the carbonyl moiety of ketene R_2CCO ($R = H$) in the beginning of the reaction. Although the reactions are concerted with $R = H$, a nucleophilic attack on diphenylketene ($R = Ph$) might yield a zwitterionic intermediate stabilized by delocalization of the negative charge within the whole diphenylenolate moiety (Scheme 3).[56] To prove this hypothesis, we have tried to localize a zwitterionic intermediate formed by an attack of $CpReO_3$ on R_2CCO on the potential-energy surfaces. The calculations reveal that the intermediate does not exist for $R = H$ but for $R = Ph$;[57] its fully optimized geometry is shown in Figure 9.[58] The coordination mode of the Cp ligand is η^5 and the phenyl rings are twisted by 12 and 53 degrees out of the enolate plane. The energy of the zwitterionic intermediate is predicted to be only 7.9 kcal/mol higher than that of the reactants; an additional stabilization

(54) Schlecht, S.; Dehnicke, K. Unpublished results.

(55) Test calculations using the improved model ligand Me_3PN instead of H_3PN led to changes of the [3+2] and [2+2] activation barriers for the cycloadditions less than 1 kcal/mol.

(56) The origin of the loss of concertedness in pericyclic reactions has recently been elucidated: Vivanco, S.; Lecea, B.; Arrieta, A.; Prieto, P.; Morao, I.; Linden, A.; Cossio, F. P. *J. Am. Chem. Soc.* **2000**, *122*, 6078.

(57) The attempts to localize a zwitterionic intermediate for the reaction of $CpReO_3$ with ketene on the potential-energy surface include optimizations starting with a geometry taken from the intermediate for the reaction of $CpReO_3$ with diphenylketene.

(58) The intermediate was calculated at the BP86/III∼ level using the ADF program, because the molecule is presently too large for geometry optimizations at the B3LYP/II level using Gaussian 98. All the stationary points for the reaction of $(NPH_3)ReO_3$ with ketene have been optimized at both levels to demonstrate that similar results are obtained (compare Figure S1 in the Supporting Information to Figure 4). A good agreement of the calculated energies at B3LYP/III+//B3LYP/II and BP86/III∼ has also been obtained for most of the stationary points (see Table S1 in the Supporting Information). The BP86 potential energy surface is systematically shifted to lower energies relative to the reactants, which is a well-documented trend in bimolecular reactions involving transition metal compounds ((a) Musaev, D. G.; Froese, R. D.; Morokuma, K. *Organometallics* **1998**, *17*, 1850). A larger difference of 9.5 kcal/mol between the energies at the two levels has been predicted for the metalla-2,5-dioxolane ([3+2] product). We have also calculated the relative energies of the [3+2] products for OsO_4 and found a reasonable agreement with the CCSD(T)/III+//B3LYP/II value; the B3LYP/III+//B3LYP/II values are lower and the BP86/III∼ values slightly higher than the CCSD(T)/III+//B3LYP/II energies (see Table S2 in the Supporting Information). Note that there is a strong basis-set dependence of the energies; the relative energies of the [3+2] products at B3LYP/II are much smaller than those calculated using improved basis sets. For additional examples for a comparison of the two functionals BP86 and B3LYP, see: (b) Reference 38. (c) Deubel, D. V. *J. Phys. Chem. A* **2001**, *105*, 4765.

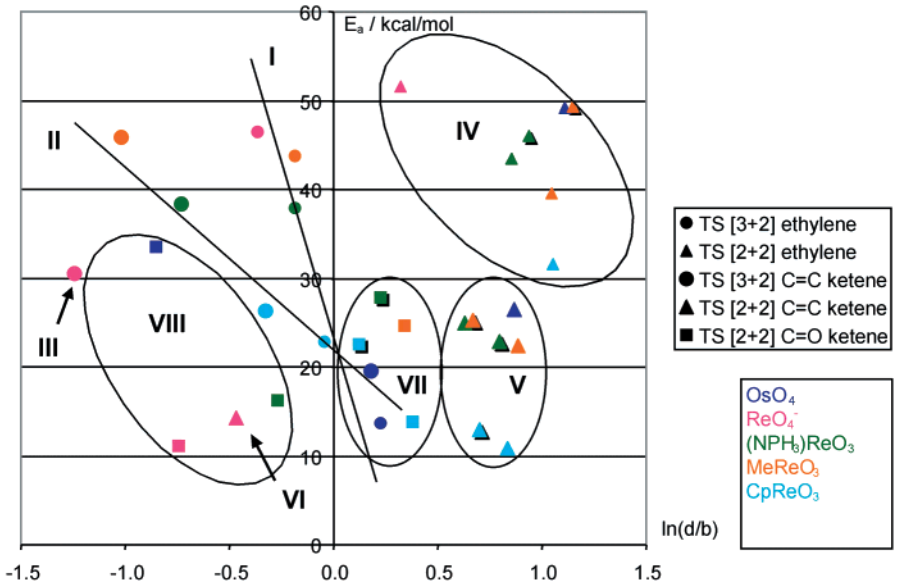

Figure 8. Plot of the activation energies E_a versus ln(d/b). If there are cis and trans isomers, the symbol for the trans configuration is shaded.

Scheme 3. Postulated Reaction Mechanism for the Addition of Metal Oxides to Diphenylketene (R = Ph)

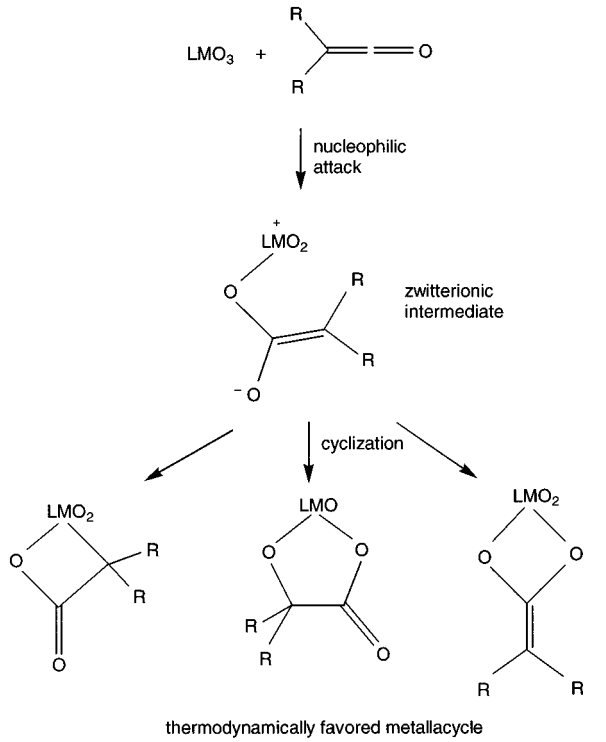

can be expected from solvation effects. The intermediate is probably formed in the rate-determining step since it has not been isolated[25,54] and the subsequent cyclization is supposed to be fast, yielding the most stable metallacycle (Scheme 3). Unfortunately, the molecules are presently too large for systematic geometry optimizations of the transition states for metal-oxide additions to diphenylketene and for a theoretical consideration of solvation effects. However, the suggested two-step mechanism is in accordance with the experimental results: In the reactions of both (R′$_3$PN)ReO$_3$[54] and Cp*ReO$_3$[25] with diphenylketene, the thermodynamically favored products are obtained, respectively. Further support of the proposed mechanism via the zwitterionic intermediate is given by the fact that MeReO$_3$ reacts with diphenylketene only in the presence of additional ligands, i.e., 1 equiv of *t*-Bu-bipy or 2 equiv of *t*-Bu-py.[26a] These ligands increase the reactivity of the metal oxide with respect to a nucleophilic attack of an oxo functionality at the carbonyl moiety of the heterocumulene.

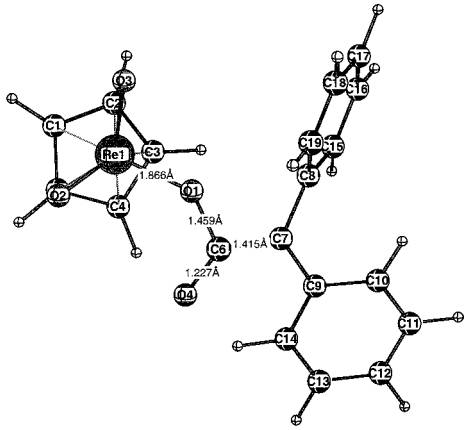

Figure 9. Optimized geometry (BP86/III~) of the zwitterionic intermediate formed by nucleophilic attack of CpReO$_3$ at the carbonyl moiety of diphenylketene.

Conclusions

(i) A [3+2]-versus-[2+2] periselectivity of the addition of metal oxides to ketene is originated by the metal. OsO$_4$ is highly electrophilic at the oxo moieties but scarcely electrophilic at the metal; it prefers the [3+2] pathway. In contrast, the rhenium oxides LReO$_3$ (L = O$^-$, H$_3$PN, Me, Cp) are O-nucleophilic and metal-electrophilic and favor [2+2] cycloadditions to ketene.

(ii) A C=C-versus-C=O chemoselectivity of the [2+2] addition of LReO$_3$ to ketene arises from the ligand L. With L = O$^-$ and H$_3$PN, the calculated C=O barrier is lowest whereas the metal oxides with the softer ligands Me and Cp favor the C=C additions to ketene. However, the differences between the calculated [2+2] activation barriers are small.

(iii) The large deviations between the calculated energy profiles for the MeReO$_3$ and CpReO$_3$ additions are due to the role of the Cp ligand as a stereoelectronic mediator. In contrast, the η^1 mode of Cp* is destabilized.

(iv) Parameters of Charge Decomposition Analysis (CDA) enable the prediction of the activation energies of [3+2] additions of metal oxides across C=C double bonds. Further-

more, CDA divides the [2+2] additions to ketene into three categories: synchronous additions across the C═C moiety, synchronous additions across the C═O moiety, and asynchronous but concerted additions predominated by a nucleophilic attack at the central carbon in the beginning of the reaction.

(v) The reactions of metal oxides with diphenylketene probably follow a different mechanism: A zwitterionic intermediate is formed by the nucleophilic attack of an oxo ligand at the carbonyl moiety. The subsequent cyclization gives the thermodynamically favored metallacycle. This two-step pathway is supported by the calculated geometry and energy of the postulated intermediate and by the results of experimental work.

Acknowledgment. We thank Prof. Dr. Kurt Dehnicke for helpful discussions. Dirk V. Deubel thanks the Fonds der Chemischen Industrie for a Kekulé Scholarship, the Deutscher Akademischer Austauschdienst for a NATO Fellowship, and the Alexander-von-Humboldt Foundation for a Feodor-Lynen Fellowship. This work has also been supported by the Deutsche Forschungsgemeinschaft. Excellent service has been provided by the computer center HRZ UNI Marburg.

Supporting Information Available: Geometries and energies for the stationary points of the reaction of $(NPH_3)ReO_3$ with ketene calculated at the BP86/III∼ level, energies for the [3+2] addition of OsO_4 to ethylene calculated at various levels of theory, Cartesian coordinates of all stationary points, and total energies in hartrees at each level of theory (PDF). This material is available free of charge via the Internet at http://pubs.acs.org.

JA003733S